[AMERICAN JOURNAL OF SCIENCE, VOL. 276, SUMMER, 1976, P. 817-840]

BIMETASOMATISM RESULTING FROM INTERGRANULAR DIFFUSION: I. A THEORETICAL MODEL FOR MONOMINERALIC REACTION ZONE SEQUENCES

JOHN D. FRANTZ and H. K. MAO

Geophysical Laboratory, Carnegie Institution of Washington, Washington, D.C. 20008

ABSTRACT. A model for prediction of the growth of monomineralic zones in one-dimensional metasomatic columns resulting from intergranular diffusion was developed. A theoretical formulation based on Fick's laws of diffusion and the local equilibrium principle can be used to calculate the sequence and thicknesses of reaction zones. The loss or production of solid phases *within* the monomineralic reaction zones and *at* the zone boundaries is related to gradients in the concentrations of the aqueous species. The total zone growth rate, however, is independent of concentration gradients and depends only on the solution concentrations at zone boundaries. A set of n simultaneous differential equations of the following form is employed for total zone growth rates:

$$dL_j/dt = \sum_{k=1}^{n} R_{jk}/L_k$$

where L_j is the thickness of the jth zone and t the time. The term $R_{jk} = 0$ when $k < j - 1$ or $k > j + 1$. The values of R_{jk} are functions of diffusion potentials, porosity, and tortuosity. Diffusion potentials (Φ_i) are defined as

$$\Phi_i\ (c_1, c_2, \ldots, c_n) = \int \sum_{h=1}^{n} D_{ih} \nabla c_h dx$$

where c_i, D_{ih}, and x represent the concentration, the diffusion coefficient, and the space coordinate. Mathematical models utilizing this variable can be used in cases when the diffusion coefficients vary with solution concentrations. Provision for changes in the volume of solids and porosity makes the model applicable to systems involving increases or reductions in total rock volume. Calculations have been made for metasomatic zone sequences for rocks related to the system $MgO–SiO_2–H_2O–HCl$.

INTRODUCTION

With the exception of volatiles such as CO_2 and H_2O, changes in most metamorphic bodies are considered to be isochemical, resulting mainly from variations in temperature and pressure. There is much evidence, however, that chemical potential gradients do exist in many such rock bodies. Carmichael (1969), Eugster (1970), and Fisher (1970) have shown that microscopic gradients often exist between neighboring minerals or mineral groups owing to temperature- and pressure-induced reactions among the solid phases. Megascopic gradients are illustrated by skarn deposits due to the emplacement of igneous intrusions and by variations in original sediment bulk composition. The extent to which the paragenesis of a rock is determined by the existence of chemical potential gradients depends upon the rates of change in temperature and pressure as opposed to the magnitude of material flux. In cases of rapid

change in temperature and pressure coupled with slow transport of material along gradients, bulk compositions remain relatively constant, and mass transport plays very little role in the rock's metamorphic evolution. With higher relative rates of material transport, however, the history of the rock body is often dependent on the mechanism of transfer of matter.

In recent years, a great deal of interest has focused on different types of transport models and their use in predicting the paths by which rock systems containing chemical potential gradients approach quasi-static equilibrium. Much of this effort has been concentrated on dissolution kinetics in which the rate of dissolution of a solid in an aqueous fluid is often dependent on diffusion of material through incongruent reaction rims. Wollast (1967) experimentally studied the alteration of potassic feldspars and found the dissolution rate to be controlled by diffusion of H_4SiO_4 through a leached residual layer of $Al(OH)_3$ and subsequent reaction of these substances to form a hydrated aluminum silicate. Helgeson (1971) used a thermochemical approach to predict dissolution reaction paths based on diffusional transport of material from the reactant mineral through a surface layer of intermediate reaction products as the rate-limiting step. Luce, Bartlett, and Parks (1972) developed a diffusion model for the dissolution of magnesium-silicate minerals which explains their experimentally observed short-term incongruency and long-term near congruency. In the studies, communication between the fluid phase and the core has been shown by O'Neil and Taylor (1967) to result from diffusion along aqueous grain boundary films within a polycrystalline reaction rim rather than from volume diffusion. These incoherent surfaces result from structural and molar volume differences between the core and rim.

The mineral dissolution mechanism is but one step in metasomatic processes occurring under metamorphic conditions. Rather than a large mass of homogeneous fluid, the grains are probably surrounded by a thin grain-boundary film which serves as the agent for intergranular transport. Recently several models have been developed to describe material transfer through these intergranular films. Two general mechanisms have been proposed: (1) diffusion through a stationary pore fluid and (2) convective transport due to motion of the pore fluid relative to the solid framework (infiltration). Korzhinskii (1970) derived transport equations for both models using them to analyze qualitatively resulting metasomatic zones. Hofmann (1972) applied the infiltration model to the alteration of feldspars using the theoretical treatment of liquid chromatography. Frantz and Weisbrod (1974) calculated the sequences and thicknesses of the metasomatic reaction zones resulting from infiltration within the K_2O–Al_2O_3–SiO_2–H_2O–HCl system. Fletcher and Hofmann (1974) developed equations useful in treating transport of one component involving both diffusion and infiltration. Fisher (1973, 1975) applied the formulation of irreversible thermodynamics to the investigation of metamorphic reaction textures resulting from intergranular diffusion. This approach utilizes relative chemical potential gradients rather than the concen-

tration gradients and assumes linear chemical potential gradients. Weare, Stephens, and Eugster (this issue, p. 767-816) have studied the hydrolysis of feldspars using a model similar to the one presented in this paper.

Essential for the understanding of natural transport processes occurring by intergranular diffusion in multicomponent systems is the development of a model by which the sequence and thicknesses of natural bimetosomatic reaction zones can be predicted quantitatively using data from laboratory experiments. With the present growing interest in the experimental determination of mineral-solution equilibria, it is now possible to calculate accurately concentration gradients within many rock systems under metamorphic conditions. Solutions of the diffusion equations, however, require knowledge of porosity, tortuosity, and diffusion coefficients, in addition to concentration gradients. The present approach is to develop a general model for calculating zone thicknesses utilizing all these parameters and then to make quantitative calculations based on the concentration gradient data available. Mineral surface effects will be neglected. (The applicability of these calculations to natural systems would then depend on the relative importance of concentration gradients over (1) differences in the diffusion coefficients of the aqueous species, and (2) changes in porosity and tortuosity.)

An extremely helpful assumption in any theoretical treatment of transport processes is the "local equilibrium" hypothesis (Korzhinskii, 1959; Thompson, 1959). This principle states that certain large systems not in equilibrium owing to gradients in intensive parameters can be approximated by a series of small subsystems, each of which is treated as an equilibrium system. Using this hypothesis, Thompson (1959) demonstrated that in metasomatic reaction sequences at constant temperature and pressure, the number of mineral phases within a zone coexisting with an intergranular fluid is two or more less than the number of components. For three-component systems involving two diffusing solutes and H_2O, only one mineral phase can coexist with the fluid.

Because one of the purposes of this model is to predict the relative thicknesses of zones, changes in rock volume due to mineral replacement must be considered. Intergranular transport in isochroic systems in which local equilibrium exists is likely only if reactions involve reduction in solid volumes or if sufficient porosity exists to accommodate any solid-volume increases (Frantz and Weisbrod, 1974). In isobaric systems involving solid volume increases not compensated by porosity, the rocks must expand if reaction is to occur. The foregoing model accommodates both solid-volume and porosity changes, making it applicable to systems involving increases or reductions of total rock volume.

In the theoretical portion of this paper, the differential equations expressing one-dimensional rates of expansion of reaction zones will be developed for monomineralic reaction columns resulting from diffusion. In the following sections, these equations are applied toward the quantitative prediction of reaction-zone thicknesses resulting from metasomatic alteration in the system MgO–SiO_2–H_2O–HCl.

THEORY

TABLE 1

Summary of symbols

A_i	The component i.
B_{x_j} zone j	The growth rate of zone j at boundary x_j.
D_{ih}	The diffusion coefficient of species i with respect to the gradient of h.
I_j	The internal growth rate of zone j.
J_i	The number of moles of aqueous species i transferred through the pores of unit area cross section of rock per unit time.
K_j	Solubility constants for mineral in jth zone.
L_j	The thickness of zone j.
M_i	The number of moles of species i in the fluid per unit volume of rock.
N_j	The number of moles of solid j in zone j.
$\bar{V}_j$	The molar volume of the solid in zone j.
a_{ij}	The stoichiometric coefficient of the component i in the mineral of the jth zone.
c_h	The molality of species h in the fluid.
m_i	The number of moles of species i in the fluid gained from reaction with the solid per unit volume of the rock per unit time.
$m_{ix_{j+1}}$*	The number of moles of species i in the fluid gained from reaction with solids at the zone boundary x_{j+1} per unit area per unit time.
n_j	The number of moles of the solid in the jth zone formed from reaction with the fluid per unit volume of the rock per unit time.
n_{x_j} * zone j	The number of moles of the solid in the jth zone formed from reaction at the zone boundary x_j per unit area per unit time.
x	The space coordinate normal to the zone boundaries.
x_j	The position of the jth boundary.
β	The porosity.
ϕ_i	The diffusion potential of species i times the porosity and tortuosity.
Φ_i	The diffusion potential of species i.
τ	The tortuosity.
$v_{x_{j+1}}$ zone j	The reaction coefficients of the solid phases in zone j at boundary j+1.

Fick's first law is a hypothesis stating that "the rate of transfer of a diffusing substance through unit area of a section is proportional to the concentration gradient measured normal to the section" (Crank, 1970). Considering diffusion through a static pore fluid in a rock:

$$J_i = \sum_{h=1}^{n} \beta\tau D_{ih} (\partial c_h/\partial x)_t \qquad (1)$$

where J_i is the rate of transfer of aqueous species i through the pores of unit cross section of rock, c_h is the concentration of species h in the fluid, x is the space coordinate measured normal to the section, τ the tortuosity factor, β the porosity, and D_{ih} the diffusion coefficient.

Assuming the porosity and tortuosity to be uniform and assuming the diffusion coefficient to be only a function of the concentrations of the solution species, the following function is defined:

$$\Phi_i\ (c_1, c_2, \ldots, c_n) = \int \sum_{h=1}^{n} D_{ih}(\partial c_h/\partial x)_t dx \qquad (2)$$

where Φ_i will be called the "diffusion potential". Combining equations (1) and (2), defining $\emptyset_{ij} = \beta_j \tau_j \Phi_i$, yields Fick's first law in terms of the diffusion potential:

$$J_i = -(\partial \phi_{ij}/\partial x)_t \qquad (3)$$

By combining Fick's laws of diffusion with the Law of Conservation of Mass, one can calculate the rate at which an aqueous species is lost or gained, with respect to time, in a small fixed volume of a mineral zone or at a boundary between two such zones. If one assumes steady-state diffusion profiles for the aqueous solutes within mineral zones, any gain or loss of material from the fluid is due to reaction with the solid phase or phases.

Within a metasomatic column produced by multicomponent intergranular diffusion of aqueous solutes under conditions of local equilibrium, production of solid material occurs both at the zone boundaries and within the monomineralic reaction zones. Consider, for example, a bimetasomatic column formed by diffusion of two aqueous species (i,h). The steady-state concentration profiles are schematically represented in figure 1. In the simplest case when $\beta_\tau D_{ii}$ equals unity and D_{ij} equals zero, the diffusion potential ϕ_i equals c_i, and the figure can be thought as a profile of ϕ. The discontinuities of the gradients at x_j and x_{j+1} indicate growth or loss of the solid phase at the zone boundaries. Concave-down discontinuities of ϕ_i indicate loss of the aqueous species from the fluid to form the solids; convex-up discontinuities indicate a gain of aqueous species by dissolving the solids. The curvature of ϕ within the

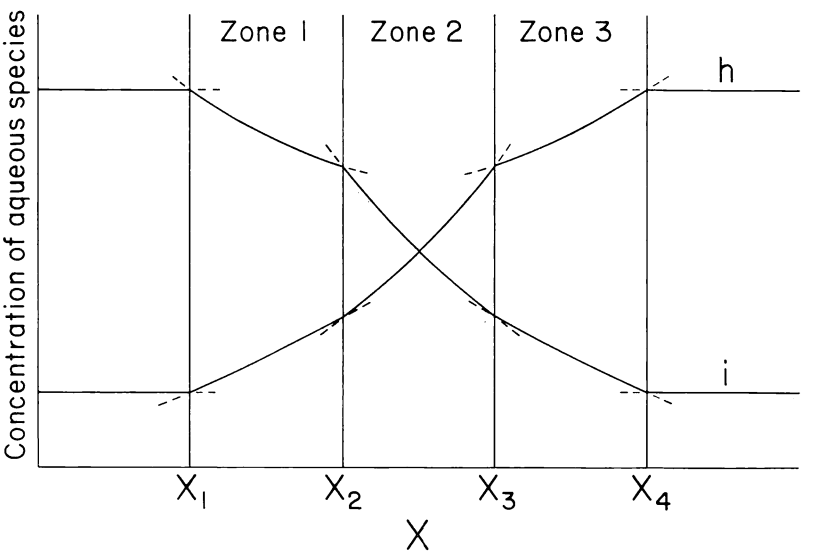

Fig. 1. Plot of the concentrations of aqueous species i and h as functions of x. The areas j—1, j, j+1 refer to monomineralic reaction zones which are separated by zone boundaries x_j and x_{j+1}. The dashed curves are metastable extensions.

zones indicates internal production or dissolution of the solid phase. Again a concave-down curvature indicates production; a convex-up curvature, dissolutions; and a straight line, neither production nor dissolution of the solids. The internal production can be explained by considering a ternary mole-fraction diagram (fig. 2). The mixing of two fluids of different compositions, both in equilibrium with a common phase, causes additional precipitation of the common solid. Consider the effect of a one-to-one mixture of solutions p and q which are both in equilibrium with phase C. This effect has long been known by solution chemists as the "salting-out" effect (Garrels and Christ, 1965). Unless sufficient porosity exists, internal production requires the zone to expand. Such increases in rock volume must occur in a manner analogous to increases at zone boundaries. As will be seen in a later section, the expansion within zones may be partially or entirely offset by rock volume decreases at the zone boundaries.

In the following sections, the loss or production of the solid phases *within* the monomineralic reaction zones and *at* the zone boundaries can

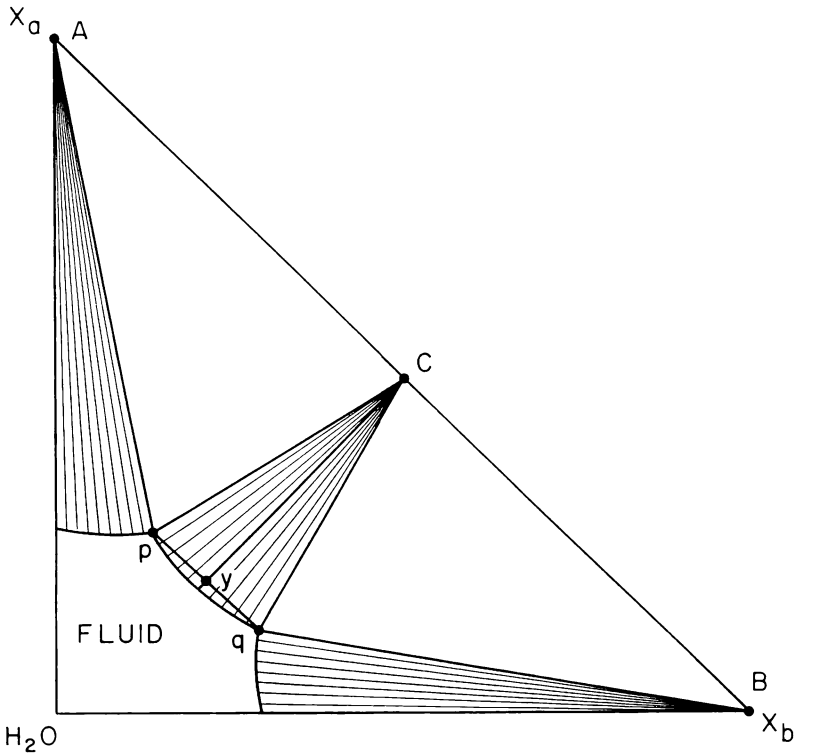

Fig. 2. Mole fraction diagram for system a–b–H_2O containing solid phases A, B, and C.

be related to changes in the diffusion potentials of the aqueous species. Resulting from this will be a model suitable for calculating changes in monomineralic reaction zone widths occurring in bimetasomatic one-dimensional columns.

Internal production within zones.—Consider a small volume whose position is fixed irrespective of movements of the rock or intergranular fluid. The Law of Conservation of Mass for the fluid portion of this small volume can be expressed as follows (Katchalsky and Curran, 1967):

$$(\partial J_i/\partial x)_t = -(\partial M_i/\partial t)_x + m_i \tag{4}$$

where M_i is the number of moles of species i in the fluid per unit volume of the rock; m_i is the number of moles of species i in the fluid lost or gained due to reaction per unit volume of rock per unit time at constant x (m_i will be considered positive for moles gained in the fluid by dissolving the solid).

Within this small volume, the number of moles of species i in the fluid per unit volume can be expressed as:

$$M_i = \beta c_i \tag{5}$$

where c_i is the molarity of aqueous species i. Differentiating equation (3) with respect to x and equation (5) with respect to time and substituting both into equation (4):

$$-(\partial^2\phi_{ij}/\partial x^2)_t = -\beta(\partial c_i/\partial t)_x + m_i \tag{6}$$

In a rock of low porosity saturated with a fluid of low concentration, the total amount of a component dissolved in the fluid is negligible in comparison with the total amount of the component in the solid. When the component is transported, the amount required to adjust the concentration of the fluid is also negligible in comparison with the amount required to produce the new solid. Therefore, within the time scale of the growth of the solid, the adjustment of the concentration of the fluid to steady state is almost instantly achieved, and the concentration profiles of aqueous species within any zone can be described by a steady-state model. Thus:

$$\beta(\partial c_i/\partial t)_x \cong 0 \tag{7}$$

and equation (6) becomes

$$(\partial^2\phi_{ij}/\partial x^2)_t = -m_i \tag{8}$$

where the subscript j indicates the function ϕ_i in the jth zone.

The loss of aqueous species i from the fluid phase m_i occurs owing to reactions with solids and with other aqueous species. Consider reactions between aqueous species and the solid phase within the monomineralic zone:

$$[(A_1)_{a_{1j}}(A_2)_{a_{2j}}\ldots]_{(solid)} = a_{1j}A_{1(aq)} + a_{2j}A_{2(aq)} + \ldots \tag{9}$$

where A_1, A_2, . . . represent components of solid phase; $A_{1(aq)}$, $A_{2(aq)}$, . . . represent components of aqueous species; and a_{ij} are the stoichiometric coefficients of these components in the mineral of the jth zone. Letting n_j equal the gain in moles of solid phase j per unit volume per unit time due to reaction at x, the following mass balance expression between solid and fluid is obtained:

$$a_{ij}n_j + m_i = 0 \tag{10}$$

Substituting equation (8) into (10) and rearranging:

$$n_j = (1/a_{ij})(\partial^2\phi_{ij}/\partial x^2)_t \tag{11}$$

which describes the rate of production of solid phase j per unit rock volume due to diffusion of aqueous species i within the intergranular fluid phase.

Integration of equation (11) with respect to x leads to an expression describing changes in the amount of the solid phase per unit area within the entire zone as a function of time. Letting x_j and x_{j+1} denote the positions of the two boundaries of the jth reaction zone:

$$I_j = \bar{V}_j \int_{x_j}^{x_{j+1}} n_j dx = (\bar{V}_j/a_{ij}) \left[(\partial\phi_{ij}/\partial x)_{x_{j+1}} - (\partial\phi_{ij}/\partial x)_{x_j} \right] \tag{12}$$

where $\bar{V}_j$ is the molar volume of solid j (porosity has been neglected) and I_j is the rate of thickness change due to internal precipitation. Thus, one can calculate the internal production within a monomineralic reaction zone by knowing the concentration gradients of any one aqueous species at both zone boundaries.

Production or loss at zone boundaries.—Concentration gradients of the fluid phase at zone boundaries are discontinuous (fig. 1), and thus we must consider conservation of mass across a plane normal to the flow direction. In this case, the following conservation equation can be written:

$$\Delta J_{ix_{j+1}} = m_{ix_{j+1}}{}^* \tag{13}$$

where ΔJ_i is the difference between the total fluxes on the two sides of the phase boundary; $m_{ix_{j+1}}{}^*$ is the number of moles of species i lost or gained at the boundary x_{j+1} per unit area per unit time due to reaction. Substituting equation (3) into (13):

$$(\partial\phi_{ij}/\partial x)_{x_{j+1}} - (\partial\phi_{i,j+1}/\partial x)_{x_{j+1}} = m_{ix_{j+1}}{}^* \tag{14}$$

As in the case of internal production, the loss or gain of aqueous species i from the fluid phase occurs owing to reaction with solids and

other aqueous species. Consider the following reaction occurring at the j+1 zone boundary:

$$v_{\substack{x_{j+1}\\ \text{zone j}}}\left[\ (A_1)_{a_{1,j}}\,(A_2)_{a_{2,j}}\cdots\ \right]_{\text{solid}} + v_{\substack{x_{j+1}\\ \text{zone j+1}}}\left[\ (A_1)_{a_{1,j+1}}\,(A_2)_{a_{2,j+1}}\cdots\ \right]_{\text{solid}} =$$

$$\sum_{i=1}^{P} A_i \left(v_{\substack{x_{j+1}\\ \text{zone j}}}\ a_{i,j} + v_{\substack{x_{j+1}\\ \text{zone j+1}}}\ a_{i,j+1} \right)_{\text{aqueous}} \qquad (15)$$

where $v_{\substack{x_{j+1}\\ \text{zone j}}}$ and $v_{\substack{x_{j+1}\\ \text{zone j+1}}}$ are the reaction coefficients of the solid phases in zones j and j+1 at boundary x_{j+1}. Considering production or loss due to reaction at the zone boundary with respect to time, one can write expressions relating the gain or loss of phase j to changes in fluid composition (per unit area):

$$\left(v_{\substack{x_{j+1}\\ \text{zone j}}}\ a_{i,j} + v_{\substack{x_{j+1}\\ \text{zone j+1}}}\ a_{i,j+1} \right) n_{\substack{x_{j+1}\\ \text{zone j}}}{}^{*} + v_{\substack{x_{j+1}\\ \text{zone j}}}\ m_{i,x_{j+1}}{}^{*} = 0 \qquad (16)$$

where $n_{\substack{x_{j+1}\\ \text{zone j}}}{}^{*}$ equals the rate at which moles of solid phase j+1 gained per unit area per unit time at zone boundary x_{j+1}. One can write such equations for each zone (one for each aqueous species). Substituting equation (14) into (16) and eliminating $v_{\substack{x_{j+1}\\ \text{zone j}}}$ and $v_{\substack{x_{j+1}\\ \text{zone j}}}$ between two such expressions, one gets relations of the following form:

$$B_{\substack{x_{j+1}\\ \text{zone j}}} = \bar{V}_j n_{\substack{x_{j+1}\\ \text{zone j}}}{}^{*} = \left(\frac{\bar{V}_j}{a_{ij}a_{h,j+1} - a_{hj}a_{i,j+1}} \right)\Bigg(a_{i,j+1}\left[\left(\partial\phi_{hj}/\partial x \right)_{x_{j+1}} - \left(\partial\phi_{h,j+1}/\partial x \right)_{x_{j+1}} \right] - a_{h,j+1}\left[\left(\partial\phi_{ij}/\partial x \right)_{x_{j+1}} - \left(\partial\phi_{i,j+1}/\partial x \right)_{x_{j+1}} \right] \qquad (17)$$

where i and h are any two aqueous species and $B_{x_{j+1}}$ is the rate of growth of zone j at boundary j+1.

Similarly, the growth or loss of phase j at boundary x is given by the relation:

$$B_{\substack{x_j\\ \text{zone j}}} = \bar{V}_j n_{x_j}{}^{*}_{\text{zone j}} = -\left(\frac{\bar{V}_j}{a_{ij}a_{h,j-1} - a_{hj}a_{i,j-1}} \right)\Bigg(a_{i,j-1}\left[\left(\partial\phi_{hj}/\partial x \right)_{x_j} - \left(\partial\phi_{h,j-1}/\partial x \right)_{x_j} \right] - a_{h,j-1}\left[\left(\partial\phi_{ij}/\partial x \right)_{x_j} - \left(\partial\phi_{i,j-1}/\partial x \right)_{x_j} \right] \qquad (18)$$

We thus have the two equations describing production or loss of solid j at the two zone boundaries of zone j owing to diffusion of aqueous species i and h.

Total zone growth.—The rate of change of moles of solid j in zone j is the sum of the rates of loss or production at the boundaries and the rate of internal growth:

$$E_j = dL_j/dt = B_{x_j}{}_{\text{zone j}} + I_j + B_{x_{j+1}}{}_{\text{zone j}} \tag{19}$$

where $L_j = x_{j+1} - x_j$ is the thickness of the jth zone.

Referring to equations (12), (17), and (18), one can see that rates of change of zone thicknesses are functions of diffusion potential gradients at the zone boundaries. When steady-state diffusion is assumed, the diffusion potential gradients of different aqueous species can be related to each other. Consider equation (11) relating production of solid phase j to the second derivatives of the aqueous concentrations at components i and h:

$$n_j = -\frac{1}{a_{ij}}(\partial^2\phi_{ij}/\partial x^2)_t = -\frac{1}{a_{hj}}(\partial^2\phi_{hj}/\partial x^2)_t \tag{20}$$

Integrating the second equality:

$$a_{hj}(\partial\phi_{ij}/\partial x)_t - a_{ij}(\partial\phi_{hj}/\partial x)_t = (a_{hj}\Delta\phi_{ij} - a_{ij}\Delta\phi_{hj})/L_j \tag{21}$$

where

$$\Delta\phi_{ij} = (\phi_{i,j})_{x_{j+1}} - (\phi_{ij})_{x_j}$$

Solving equations (12), (17), (18), (19), and (21), the rate of total zone growth can be reduced to an expression involving only stoichiometric coefficients, molar volumes, and zone boundary diffusion potentials

$$\begin{aligned} dL_j/dt = &-(S_1\Delta\phi_{h,j-1} + S_2\Delta\phi_{i,j-1})/L_{j-1} \\ &+ [(S_1 + S_3)\Delta\phi_{hj} + (S_2 + S_4)\Delta\phi_{ij}]/L_j \\ &-(S_3\Delta\phi_{h,j+1} + S_4\Delta\phi_{i,j+1})/L_{j+1} \end{aligned} \tag{22}$$

where S_1, S_2, S_3, and S_4 are functions of the stoichiometric coefficients and molar volume of the solid phase and are different for each zone.[1] Diffusion potential gradients $(\partial\phi/\partial x)$ at zone boundaries are not required, only values of the diffusion potentials (ϕ_{ij}). Note that the rate of zone growth is dependent on the thicknesses of neighboring zones as well as its own width.

Equations (12), (17), and (18), necessary for the calculation of the rates of internal production and boundary growth or loss, cannot be simplified and *do* require knowledge of the diffusion potential gradients at the zone boundaries. To define totally the diffusion potential profiles of the aqueous species, a mass action equation of the following form must be considered in addition to equations like (21):

$$\prod_{i=1}^{n} c_i^{a_{ij}} = K_j \tag{23}$$

---

[1] Footnote

$$S_1 = \frac{\bar{V}_j a_{i,j-1}}{a_{i,j-1}a_{hj} - a_{h,j-1}a_{ij}}, \qquad S_2 = \frac{-\bar{V}_j a_{h,j-1}}{a_{i,j-1}a_{hj} - a_{h,j-1}a_{ij}},$$

$$S_3 = \frac{\bar{V}_j a_{i,j+1}}{a_{ij}a_{h,j+1} - a_{hj}a_{i,j+1}}, \qquad S_4 = \frac{-\bar{V}_j a_{h,j+1}}{a_{ij}a_{h,j+1} - a_{hj}a_{i,j+1}}.$$

where K_j is the solubility constant for the mineral in the jth zone. A general solution for boundary diffusion potential gradients is given in the appendix.

AN EXAMPLE: BIMETASOMATISM IN THE SYSTEM $MgO–SiO_2–H_2O–HCl$

As a demonstration of the use of the preceding theoretical model, calculations have been made predicting the relative thicknesses of monomineralic reaction zones occurring by intergranular diffusion in the system $MgO–SiO_2–H_2O–HCl$. As previously stated, the present approach is to base calculations on concentration gradient data making simplifying assumptions concerning diffusion coefficients and porosities. Frantz and Eugster (1973) and Frantz (1974) have determined solubility constants for talc, serpentine, forsterite, and brucite in chloride solutions at 1000 bars between 400° and 700°C. Weill and Fyfe (1964) and Anderson and Burnham (1965) have determined the solubility of quartz in the hydrothermal environment. Using these data and assuming a fixed total concentration of chloride in the fluid independent of x, one can calculate solution concentration gradients within reaction-zone columns involving magnesium-silicate minerals. The species $MgCl_2$, H_4SiO_4, HCl, and H_2O are assumed to be the major species in the intergranular film. Only the stoichiometric phases quartz, talc, serpentine, forsterite, and brucite will be considered.

Assuming that there are no solid sinks or sources for chlorine, the four-component system $MgO–SiO_2–H_2O–HCl$ can be considered as ternary with the total chlorine concentration being fixed. Internally produced infiltration due to the formation of hydrous solid phases will be neglected. Because solution compositions are invariant at zone boundaries, the rate of change of n reaction-zone thicknesses can be expressed by n equations of the following form:

$$dL_j/dt = R_{j,j-1}/L_{j-1} + R_{j,j}/L_j + R_{j,j+1}/L_{j+1} \qquad (24)$$

where $R_{j,j-1}$, $R_{j,j+1}$ are constants independent of the zone thicknesses (see eq 22).

General analytical solutions.—General analytical solutions to the above set of differential equations have the following boundary conditions:

$$L \geqq 0 \text{ at } t = 0 \qquad j = 1,n \qquad (25)$$

Consider the growth of only one reaction zone such as the formation of a talc layer between quartz and forsterite at temperatures above the stability of serpentine. The rate of growth of the talc zone can be expressed by the following relation (simplified form of eq 24).

$$dL_{talc}/dt = R_{11}/L_{talc} \qquad (26)$$

The general solution of this ordinary differential equation is a parabolic function of the form:

$$L_{talc} = (2R_{11}t + C)^{1/2} \qquad (27)$$

where C (the integration constant) must be evaluated according to the initial reaction-zone thickness at t = 0. Equation (26) is, of course, useful only in cases when measured diffusion coefficients, porosities, and tortuosities are known and one wishes to calculate zone thickness as a function of time.

General solutions for multizone metasomatic columns, however, are much more complicated and normally not parabolic functions. The solution for a system of two reaction zones is shown in footnote 2. The complexity increases tremendously with the number of reaction zones. For a system with more than two reaction zones, general analytical solutions are impractical. The problem is approached by obtaining particular analytic solutions for special boundary conditions or by numerical methods as shown in the following sections.

Particular analytic solutions.—In many natural systems involving isothermal diffusion, bimetasomatic columns develop from initial reaction zones of zero width. Particular solutions of the differential equations (eq 24) having the following boundary conditions are, therefore, most important:

$$L_j = 0 \text{ at } t = 0 \qquad j = 1,n$$

The particular solution for the thickness of the jth reaction zone in a multizone column of n zones is the following parabolic function:

$$L_j = \left(\frac{2 \sum_{k=1}^{n} r_k R_{j,k}}{r_j} t \right)^{1/2} \tag{28}$$

where $R_{j,k}$ is constant when k = j − 1, j, or j + 1, and is zero when k assumes other values; $r_1, r_2, \ldots, r_n$ are constants and satisfy the following relationships:

$$\frac{r_{j+1}}{r_j} = \frac{\sum_{k=1}^{n} (r_k R_{j,k})}{\sum_{k=1}^{n} (r_k R_{j+1,k})} \quad (n-1 \text{ relations}) \tag{29}$$

$$r_n = 1$$

---

[2] Footnote

$$\frac{(L_1 + bL_2)^b}{(L_1 + b'L_2)^{b'}} \left(\frac{(L_1 + b'L_2)}{(L_1 + bL_2)} \right)^{R_{21}/R_{22}} = c_1$$

$$R_{22}R_{21}L_1^2 - 2R_{12}R_{22}L_1L_2 + R_{11}R_{12}L_2^2 = 2(R_{12} + R_{21})(R_{11}R_{22} - R_{21}R_{12})t + c_2$$

where:

$$b = \frac{(R_{21} - R_{12}) + \sqrt{(R_{21} - R_{12})^2 + 4R_{11}R_{22}}}{2R_{22}}$$

$$b' = \frac{(R_{21} - R_{12}) - \sqrt{(R_{21} - R_{12})^2 + 4R_{11}R_{22}}}{2R_{22}}$$

Combining the equations of (28) and (29), the following relation is apparent:

$$r_1L_1 = r_2L_2 = \ldots = L_n \tag{30}$$

which leads to the important conclusion that in ternary rock systems in which bimetasomatic columns develop from initial reaction zones of zero width by binary diffusion, *the ratio of the thicknesses at any two reaction zones is constant and independent of time.*

If D_{ii}, porosity, and tortuosity are assumed to be independent of x and concentration and if values of D_{ih}* ($i \neq h$) equal zero, the function describing the diffusion potential for any value of x is as follows:

$$\phi_i = D_i c_i \tag{31}$$

where $D_i = D_{ii}\tau\beta$ = constant. Using these assumptions, rates of zone growth in bimetasomatic columns in the system MgO–SiO_2–H_2O–HCl have been calculated.

Consider a column consisting of talc and serpentine reaction zones developing between rocks composed of quartz and forsterite at 1000 bars. Solving equations (28) and (29), the zone growth rates and thickness ratios were calculated at 380°, 400°, and 420°C (table 3). Diffusion coefficients of $MgCl_2$, H_4SiO_4, and HCl were varied, though D_{HCl} was always made equal to D_{MgCl_2} in order that the total chloride concentration be kept constant throughout the column. The boundary solution concentrations, assuming total chloride concentration equal to 1 molal, are given in table 2. The reaction zone widths (solid lines) at 400°C, assuming all diffusion coefficients equal to unity, are shown as functions of $t^{1/2}$ in figure 3.

Next consider the hypothetical case of reaction between quartz (Q) and brucite (B) yielding reaction zones composed of talc (T), serpentine (S), and forsterite (F). Again, zone growth rates and zone width ratios were calculated for different temperatures and diffusion coefficients at 1000 bars pressure (table 3). These growth rates are substantially different from those in the quartz–talc–serpentine–forsterite column (fig. 3). In figure 4, the concentration gradients at H_4SiO_4 and $MgCl_2$ are plotted against x for a Q|T|S|F|B column at 380°. The diffusion coefficients of H_4SiO_4 and $MgCl_2$ are 0.05 and 1.0 respectively ($\Delta\phi_{H_4SiO_4}$ and $\Delta\phi_{MgCl_2}$ are of the same order of magnitude). Notice that all concentration pro-

TABLE 2

Solution concentrations* at zone boundaries

Boundary	380°C		400°C		420°C	
	$C_{H_4SiO_4}$	C_{MgCl_2}	$C_{H_4SiO_4}$	C_{MgCl_2}	$C_{H_4SiO_4}$	C_{MgCl_2}
Q|T	0.02495	0.49784	0.02787	0.49691	0.03097	0.49566
T|S	0.00243	0.49954	0.00297	0.49930	0.00359	0.49897
S|F	0.00028	0.49978	0.00098	0.49952	0.00324	0.49900
F|B	0.00006	0.49985	0.00006	0.49976	0.00007	0.49962

* $C_{H_4SiO_4}$ and C_{MgCl_2} are the moles of H_4SiO_4 and $MgCl_2$ per 1000 g H_2O (molarity).

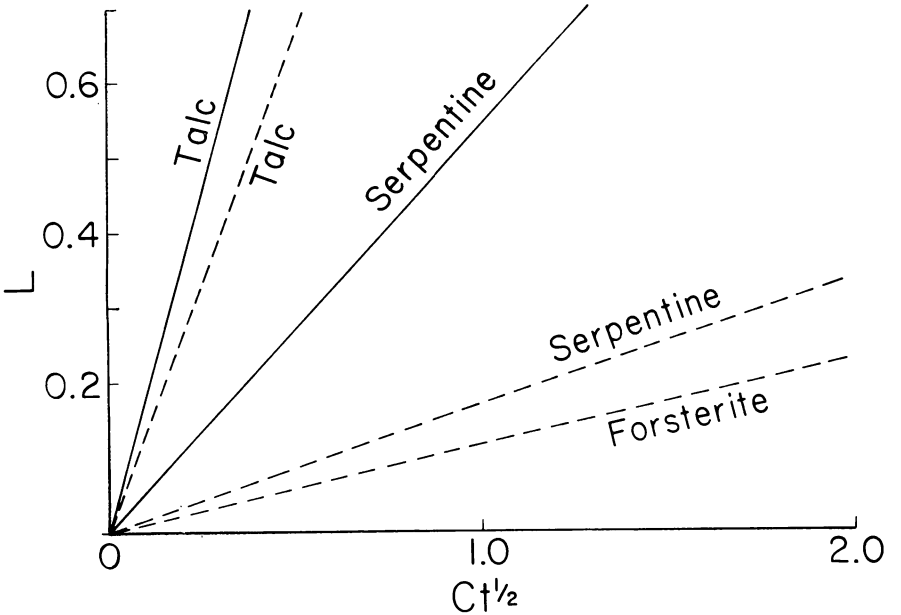

Fig. 3. Reaction zone thicknesses as functions of the square root of time ($t^{1/2}$). The solid lines refer to zones in the column quartz–talc–serpentine–forsterite; the dashed lines, to zones in the column quartz–talc–serpentine–forsterite–brucite. C is a scale factor.

TABLE 3

Reaction-zone thickness ratios

Column	T, °C	$D_{H_4SiO_4}$	D_{MgCl_2}	E_{talc}*	E_{serp}*	E_{fors}*	L_{talc}/L_{serp}	L_{talc}/L_{fors}
Q|T|S|F	380	10^{-6}	1.0	0.480	0.132	NA†	3.647	NA
		1.0	1.0	1.570	0.554	NA	2.847	NA
		1.0	10^{-6}	1.502	0.538	NA	2.790	NA
	400	10^{-6}	1.0	0.577	0.109	NA	5.274	NA
		1.0	1.0	1.690	0.502	NA	3.361	NA
		1.0	10^{-6}	1.585	0.491	NA	3.225	NA
	420	10^{-6}	1.0	0.691	0.018	NA	38.696	NA
		1.0	1.0	1.864	0.104	NA	17.820	NA
		1.0	10^{-6}	1.720	0.104	NA	16.433	NA
Q|T|S|F|B	380	10^{-6}	1.0	0.373	0.047	0.014	7.986	26.000
		1.0	1.0	1.227	0.205	0.030	5.969	40.42
		1.0	10^{-6}	1.168	0.200	0.027	5.846	42.798
	400	10^{-6}	1.0	0.441	0.036	0.038	12.341	11.470
		1.0	1.0	1.293	0.173	0.109	7.46	11.848
		1.0	10^{-6}	1.213	0.171	0.102	7.095	11.876
	420	10^{-6}	1.0	0.516	0.005	0.082	105.618	6.319
		1.0	1.0	1.348	0.027	0.311	49.172	4.337
		1.0	10^{-6}	1.246	0.027	0.302	45.443	4.126

* E_{talc} = talc zone growth rate.
E_{serp} = serpentine zone growth rate.
E_{fors} = forsterite zone growth rate.
† Not applicable.

files exhibit curvature, indicating internal production in all zones. When the diffusion concentrations of H_4SiO_4 and $MgCl_2$ are greatly different, however, the system can be approximated by one-component diffusion. In figure 5, the diffusion coefficient for H_4SiO_4 (1.0) is much higher than that of $MgCl_2$ (10^{-6}), resulting in a reaction column formed mainly by diffusion of silicic acid. Notice that the concentration gradients of the mobile component, H_4SiO_4, are nearly linear, and those of the inert component, $MgCl_2$, are curved. In this case, internal production is insignificant (eq 12). In figure 6, the roles of H_4SiO_4 and $MgCl_2$ are reversed with $D_{H_4SiO_4} = 10^{-6}$ and $D_{MgCl_2} = 1.0$. Again, internal production is insignificant, and the concentration gradients of the mobile species ($MgCl_2$) are linear. Notice by comparing the widths of zones in figures 4, 5, and 6 that large variations in relative diffusion coefficients do not cause large relative zone-thickness changes. Thus, for constant but unknown diffusion coefficients, the zone-width ratios can be quantitatively bracketed by knowing only the solution compositions at the boundaries. Zone width ratios are, however, greatly affected by changes in boundary concentrations and thus by temperature variations (table 3). The effect of varying total chloride is much the same as that of varying the diffusion coefficient of $MgCl_2$. Variation of total chloride varies the absolute $MgCl_2$ concentration differences between zone boundaries, but ratios of relative differences between sets of zone boundaries remain approximately the same.

Particular solutions by iterative methods.—As previously shown, analytical solutions for multizone columns developing from initial reaction zones of non-zero width at $t = 0$ are quite complicated. Thus, the authors have chosen to solve such problems with an iterative technique using a computer. After specifying initial reaction-zone widths, a series of new zone widths are calculated with each small successive increment in time.

Consider the bimetasomatic column quartz–talc–serpentine–forsterite at 400°, 1000 bars, with the following boundary conditions:

$$\left.\begin{aligned} L_{talc} &= 0.1 \\ L_{serpentine} &= 0.1 \end{aligned}\right\} \text{ at } t = 0 \tag{32}$$

The reaction zone thicknesses (solid lines) resulting from this particular solution are plotted as functions of $t^{1/2}$ in figure 7. Also plotted are the parabolic functions representing the reaction-zone thicknesses of a quartz–talc–serpentine–forsterite column (dashed lines) where the initial zone thicknesses are equal to zero at $t = 0$. Notice that the zone thicknesses of the column with the boundary conditions of eq (32) approach those of the parabolic functions quite quickly and are identical at infinite time.

The preceding analytical and numerical methods can be applied toward the prediction of more complicated multizone systems. Consider, for example, the development of reactions due to the presence of a quartz vein in a dunite at 400°C, 1000 bars.

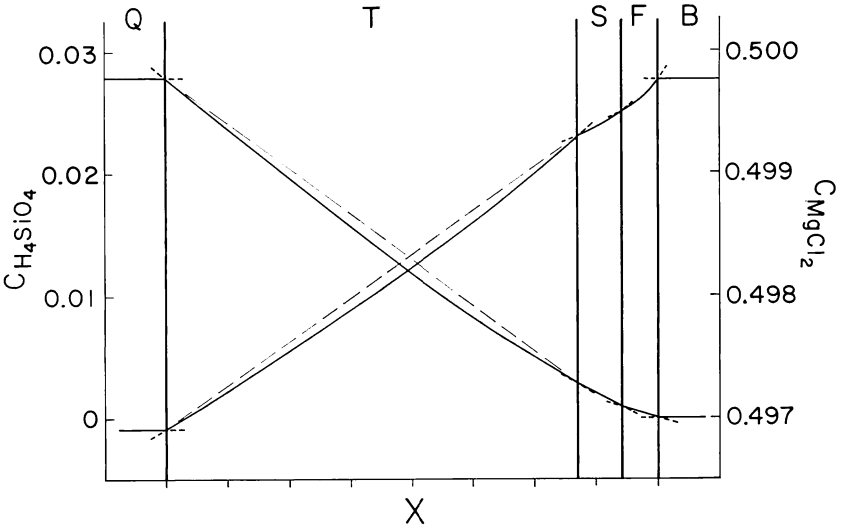

Fig. 4. Concentration profiles of $MgCl_2$ and H_4SiO_4 in Q|T|S|F|B metasomatic column at 380°C. $D_{H_4SiO_4} = 0.05$; $D_{MgCl_2} = 1.0$. The short dashed lines indicate metastable extensions. The long dashed lines are included to show curvature of profiles. Since D is constant, this figure can also be viewed as profiles of diffusion concentration (ϕ).

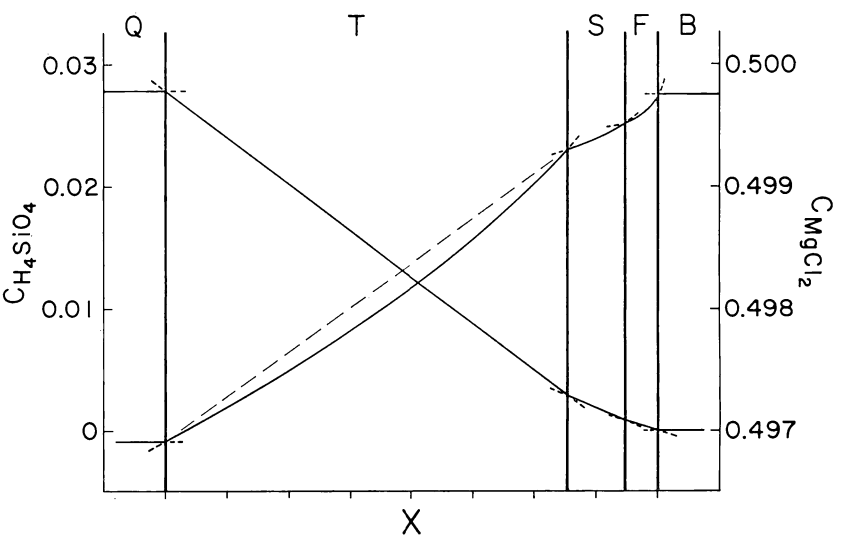

Fig. 5. Concentration profiles of $MgCl_2$ and H_4SiO_4 in Q|T|S|F|B column at 380°C. $D_{H_4SiO_4} = 1.0$, $D_{MgCl_2} = 10^{-6}$. See figure 4 for further explanation.

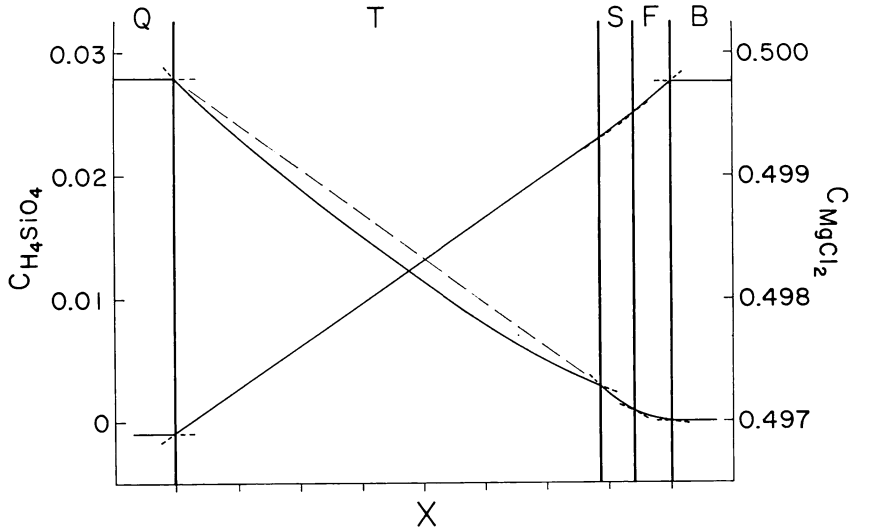

Fig. 6. Concentration profiles of $MgCl_2$ and H_4SiO_4 in Q|T|S|F|B column at 380°C. $D_{H_4SiO_4} = 10^{-6}$; $D_{MgCl_2} = 1.0$. See figure 4 for further explanation.

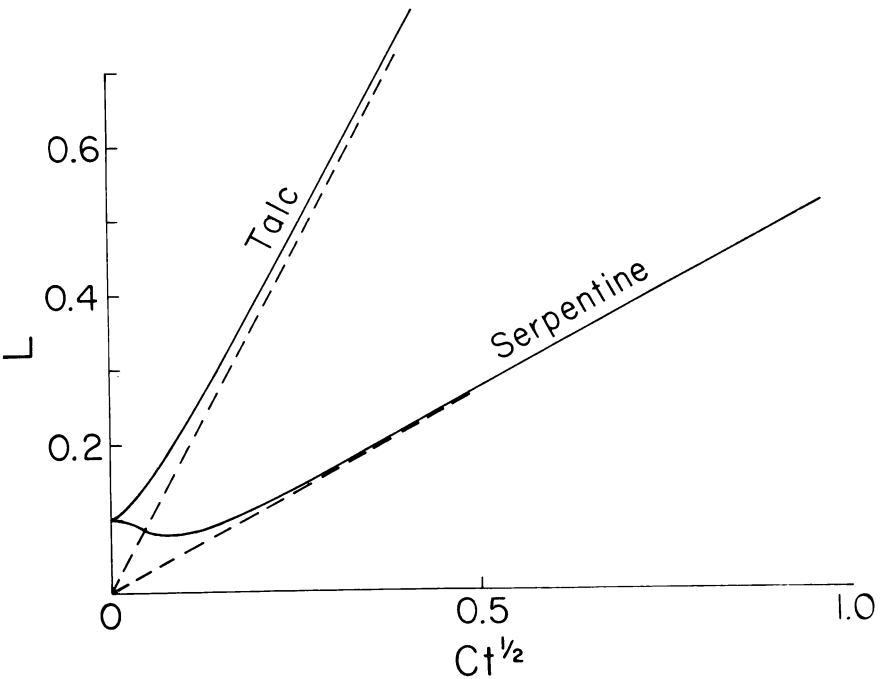

Fig. 7. Reaction zone thicknesses as functions of the square root of time for the column quartz–talc–serpentine–forsterite. The dashed lines refer to predictions based on initial reaction zone thicknesses of zero width at t = 0 (see fig. 3). The solid lines refer to predictions based on initial thicknesses at t = 0 of 0.1 cm and 0.1 cm for the talc and serpentine zones, respectively. C is a scale factor.

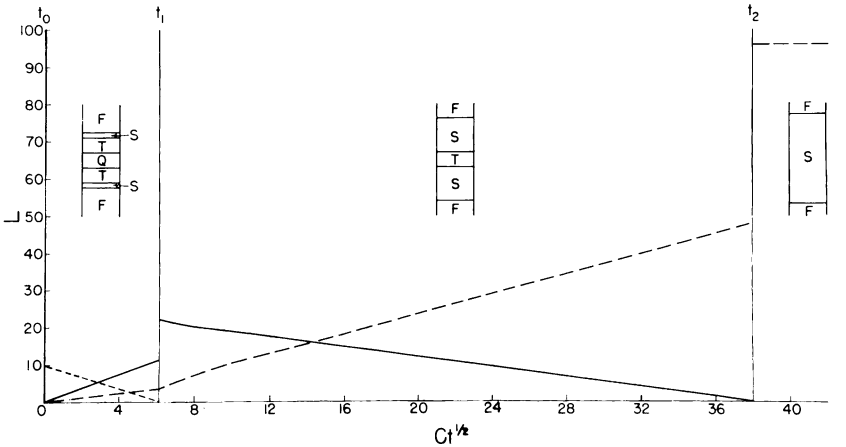

Fig. 8. Reaction zone thicknesses resulting from alteration of a quartz vein of a thickness equal to 10 in a dunite. See text for details. C is a scale factor.

Assuming the following boundary conditions:

$$\left.\begin{aligned} L_{talc} &= 0 \\ L_{serpentine} &= 0 \\ L_{quartz} &= 10 \end{aligned}\right\} \text{ at } t = 0 \qquad (33)$$

The reaction path and relative thicknesses of the reaction zones are shown in figure 8. In the initial period, the width of the quartz zone diminishes as reaction zones of talc and serpentine form on either side of the original vein. The ratio of their thicknesses corresponds to the ratio found in the particular parabolic solution of the quartz–talc–serpentine–forsterite column.

At time (t_1), the quartz zone is gone, the combined talc zone (after the quartz zone has disappeared, the talc zones on either side combine to form one zone) begins to disappear, and the serpentine zone width continues to increase, but at a different rate, which can be represented by the general parabolic solution for the development of a single reaction zone (similar to eq 27). At t_2, the talc zone disappears, and growth of the serpentine zone ceases.

Relative importance of internal growth.—As previously stated, the growth of reaction zones results from reaction both at the boundaries and within the zones. This behavior is a consequence of the local equilibrium principle. The relative contributions of zone boundary growth (B_{total}) and internal production (I) to the total growth (E_{serp}) of the serpentine zone in the Q|T|S|F|B column at 380°C are shown in table 4. Note that the ratio of internal growth to total zone growth (I/E) reaches a maximum value of 2.26 when $D_{H_4SiO_4} = 0.05$. Under these conditions, the diffusion potential of H_4SiO_4 is approximately equal to that of $MgCl_2$. At higher or lower values of $D_{H_4SiO_4}$, the contribution of internal production decreases (fig. 9) but is still quite significant (100 percent of growth rate)

when one diffusion coefficient varies by two orders of magnitude. When it varies over four orders of magnitude, internal production is of minimal significance (I/E $<$ 5 percent).

The range in which internal growth is insignificant corresponds to the range that the system can be approximated by one-component diffusion. As seen by the dashed line in figure 9, calculations based on one-component diffusion will yield zone ratios within 0.5 percent of those calculated by the bimetasomatic model in the range I/E $<$ 5 percent (outside the range between -2 and 2 on the horizontal axis).

In cases in which internal growth is large, the total boundary growth (B_{total} in table 4) is often negative. Such a case can be seen in figure 10 where $D_{H_4SiO_4} = 0.03$ and $D_{MgCl_2} = 1.0$. The serpentine is lost at the talc–serpentine boundary at a rate greater than it is gained at the serpentine–forsterite boundary resulting in a net zone boundary loss. This is compensated by a large rate of internal growth giving a positive total growth rate. As previously stated, a portion of the volume increase due to internal production is compensated by a negative net boundary growth.

Diffusion coefficients as functions of concentration.—The diffusion potential can be thought of as the effective concentration for diffusion in a manner analogous to activity being thought of as the effective concentration for chemical reaction. The diffusion potentials at zone boundaries constitute the only variables needed for the calculation of total zone growth rates. The rates of internal production and boundary growth require knowledge of the solution concentration profiles but can be also expressed in terms of ϕ. The present use of the diffusion potential variable greatly simplifies the derivation of total zone growth-rate functions in which the diffusion coefficients vary with solution concentrations. Functions of ϕ, calculated from equations relating diffusion coefficients to concentrations, can be substituted into the general zone growth rate

TABLE 4

Internal and boundary growth in serpentine zone at 380°C

$D_{H_4SiO_4}$*	I†	B_{talc}†	B_{fors}†	B_{total}†	E_{serp}†	I/E
1.0	0.134	—0.918	0.991	0.072	0.206	0.65
0.5	0.165	—0.650	0.634	—0.016	0.149	1.11
0.1	0.174	—0.259	0.165	—0.094	0.080	2.18
0.075	0.162	—0.213	0.124	—0.089	0.073	2.22
0.05	0.145	—0.160	0.079	—0.081	0.064	2.26
0.03	0.116	—0.101	0.042	—0.059	0.057	2.05
0.01	0.052	—0.003	0.003	—0.000	0.052	1.00
0.003	0.020	0.039	—0.012	0.028	0.047	0.42

* $D_{MgCl_2} = D_{HCl} = 1.0$.

† $L_{serp} = E_{serp}t^{1/2}$.
I = internal growth rate.
B_{talc} = growth rate at talc boundary.
B_{fors} = growth rate at forsterite boundary.
$B_{total} = B_{talc} + B_{fors}$ (total growth rate at boundary).
$E_{serp} = B_{total} + I$ (total growth rate).

(eq 22). ϕ will always be of the form of a constant times some function of c. In the example previously discussed, the diffusion coefficients equaled constants with no cross terms. In this case the diffusion potentials were simply the constant diffusion coefficients times the concentrations. Fisher (1976) considers another case in which $D_i = \boldsymbol{L}/c_i$ where $\boldsymbol{L}$ is a constant:

$$(\partial\phi_i/\partial x)_t = \boldsymbol{L}/c_i(\partial c_i/\partial x) \tag{34}$$

Integration yields:

$$\phi = \boldsymbol{L}\,\mathrm{Ln}\,c_i \tag{35}$$

Equation (34) could be substituted into equation (2), thereby giving a function of the zone growth rates in which D varies inversely with concentration. Cross-coefficients do not present a problem either. Assuming the following hypothetical functions for example:

$$\begin{aligned} D_{11} &= c_1 \\ D_{12} &= c_1c_2 \end{aligned} \tag{36}$$

Then,

$$\phi_1 = 1/2(c_1^2 + c_1c_2^2) \tag{37}$$

whereby the values of ϕ_i at the boundaries are completely defined by concentrations and can be used for zone growth-rate calculations. Thus, the solution for total zone growth rates given by equation (22) is totally

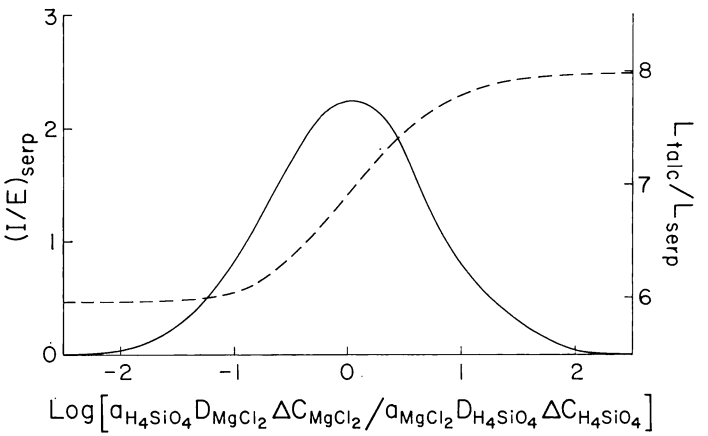

Fig. 9. Ratios of the internal growth rate to total rate (solid curve) for the serpentine zone and the ratio of talc to serpentine zone thicknesses (dashed curve) for the Q|T|S|F|B column at 380°C. I is the rate of internal growth; E is the rate of total growth; L_{serp} is the thickness of the serpentine zone; L_{talc} is the talc zone thickness. At the left end, L_{talc}/L_{serp} approaches 5.846, the limiting value for H_4SiO_4 to be the only mobile species; at the right end, L_{talc}/L_{serp} approaches 7.986, the limiting value for $MgCl_2$ to be the only mobile species. Since D is constant, the horizontal axis is equivalent to $\log(-a_{H_4SiO_4}\Delta\phi_{MgCl_2}/a_{MgCl_2}\Delta\phi_{H_4SiO_4})$, a measure of relative fluxes of $MgCl_2$ and H_4SiO_4, where $a_{H_4SiO_4}$ equals 2; and a_{MgCl_2} equals 3. See text for further details.

general for any form of diffusion coefficients as long as they are only functions of concentrations.

CONCLUSIONS

The development of a theoretical transport model suitable for predicting bimetasomatic reaction columns resulting from intergranular diffusion is an important step toward the understanding of non-isochemical rock systems. We now have a mathematical model from which the rates of growth of monomineralic reaction zones in multizone systems can be calculated. Zone growth is considered to occur both at zone boundaries and within zones. The total zone growth rates were found to be independent of concentration profiles inside the zone and dependent only on the diffusion potentials at the zone boundaries. The individual growth rates at the boundaries and within the zones, however, are dependent on concentration profiles.

Calculations of reaction zone columns in the system MgO–SiO_2–HCl–H_2O yielded information concerning the effect of internal production

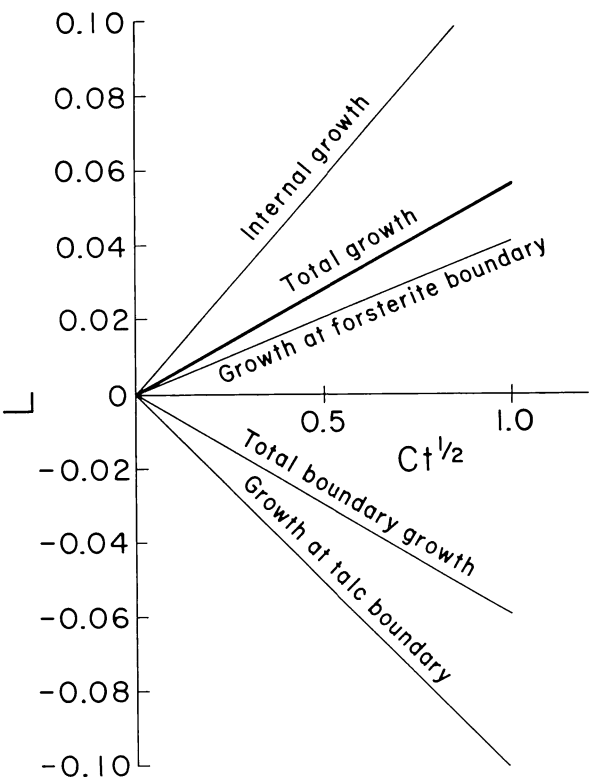

Fig. 10. Internal boundary and total growth rates as function of $Ct^{1/2}$ for serpentine zone in Q|T|S|F|B column at 380°C. $D_{H_4SiO_4} = 0.03$; $D_{MgCl_2} = 1$.

on the total zone growth rate. It was found that if the thicknesses of reaction zones in a ternary system are equal to zero at t=0, the ratios of any two zone thicknesses are constant and independent of time. The growth rates were found to be parabolic in this case. If not equal to zero, the zone growth rates soon approached those of parabolic growth.

When the changes in diffusion potentials across a zone are of the same order of magnitude for the different species, the internal growth rate was found to be significant (over two times the total growth rate). In cases when the diffusion potentials varied over 4 orders of magnitude, internal growth was insignificant, and the system could be calculated using a one-component model. The diffusion potential (ϕ_i) was found to be a useful concept for deriving general total growth-rate functions involving diffusion coefficients which are dependent on concentrations of all aqueous species.

With the use of various sets of input data, comparisons of predicted reaction columns with those found in natural rock systems should provide a basis for determining which parameters are important in controlling the paths by which non-equilibrium systems approach quasi-static equilibrium.

ACKNOWLEDGMENTS

The authors wish to thank Drs. John Brady, George Fisher, Albrecht Hofmann, Douglas Rumble, Alan Thompson, and Hatten S. Yoder, Jr., for their many helpful comments. The programming help provided by Dr. Larry Finger is greatly appreciated. Marjorie Imlay patiently typed the manuscript.

Appendix

Gradients of diffusion concentration of aqueous species, $(\partial \emptyset/\partial x)_t$, at zone boundaries

With the assumption of steady state, the second derivatives of diffusion concentrations of various aqueous species are related to each other by the stoichiometric coefficients of the solid in the jth zone:

$$a_{ij}(\partial^2\phi_{kj}/\partial x^2)_t = a_{kj}(\partial^2\phi_{ij}/\partial x)_t \tag{A1}$$

Integrating:

$$(\partial\phi_{kj}/\partial x)_t - \frac{a_{kj}}{a_{ij}}\ (\partial\phi_{ij}/\partial x)_t = \frac{Q_{kij}}{a_{ij}L_j} \tag{A2}$$

where $Q_{hij} = a_{ij}\Delta\phi_{kj} - a_{kj}\Delta\phi_{ij}$ is the integration constant. Substituting equation (3) into (A2), we obtain n equations of the following form, with k = 1 to n.

$$\sum_{h=1}^{n} \beta\tau D_{hk}^{*}\ (\partial c_h/\partial x)_t - \frac{a_{kj}}{a_{ij}}\ (\partial\phi_{ij}/\partial x)_t = \frac{Q_{kij}}{a_{ij}L_j} \tag{A3}$$

The differential form of the mass reaction equation is:

$$\sum_{h=1}^{h} \frac{a_{hj}}{c_h}\ (\partial c_h/\partial x)_t = 0 \tag{A4}$$

Combining equations (A3) and (A4) we have a set of n + 1 linear equations for n + 1 unknowns, $(\partial c_h/\partial x)_t$ with h = 1 to n and $(\partial \phi_{ij}/\partial x)_t$. The set of linear equations can be represented by the following matrices:

$$B\{(\partial c_1/\partial x)_t\ (\partial c_2/\partial x)_t \ldots (\partial c_n/\partial x)_t\ \frac{1}{a_{ij}}\ (\partial \phi_{ij}/\partial x)_t\}$$

$$= \{\frac{Q_{1ij}}{a_{ij}L_j}\ \frac{Q_{2ij}}{a_{ij}L_j}\ \ldots\ \frac{Q_{nij}}{a_{ij}L_j}\ \ 0\} \qquad \text{(A5)}$$

where the curled brackets indicate column matrices of order (n+1) × 1, and B is a square matrix of order (n+1) × (n+1) with the element at the kth row and the hth column

$$\begin{aligned} b_{kh} &= \beta\tau D_{hk}^* && \text{when } h \leq n \text{ and } k \leq n \\ b_{kh} &= a_{hj}/c_h && \text{when } h \leq n \text{ and } k = n+1 \\ b_{kh} &= -a_{kj} && \text{when } h = n+1 \text{ and } k \leq n \\ \text{and} \quad b_{kh} &= 0 && \text{when } h = k = n+1 \end{aligned} \qquad \text{(A6)}$$

Solving (A5)

$$(\partial \phi_{ij}/\partial x)_t = \frac{|B_i|}{L_j|B|} \qquad \text{(A7)}$$

where |B| is a determinant with the identical elements as the matrix B, and $|B_i|$ is a determinant with the same elements as the matrix B except

$$b_{kh} = Q_{kij} \qquad \text{when } h = n+1 \text{ and } k \leq n.$$

At zone boundaries, $(\partial \phi_{ij}/\partial x)_t$ can be calculated from $|B_i|$ and |B| which are explicit functions of stoichiometric coefficients, diffusion coefficients, concentrations of aqueous species, porosity, and tortuosity at boundaries.

References

Anderson, G. M., and Burnham, C. W., 1965, The solubility of quartz in supercritical water: Am. Jour. Sci., v. 263, p. 494-511.

Carmichael, D. M., 1969, On the mechanism of prograde metamorphic reactions in quartz-bearing pelitic rocks: Contr. Mineralogy Petrology, v. 20, p. 244-267.

Crank, J., 1970, The Mathematics of Diffusion: London, Oxford Univ. Press, 347 p.

Eugster, H. P., 1970, Thermal and ionic equilibria among muscovite, K-feldspar and aluminosilicate assemblages: Fortschr. Mineralogie, v. 47, p. 106-123.

Fisher, G. W., 1970, The application of ionic equilibria to metamorphic differentiation: an example: Contr. Mineralogy Petrology, v. 29, p. 91-103.

———— 1973, Nonequilibrium thermodynamics as a model for diffusion-controlled metamorphic processes: Am. Jour. Sci., v. 273, p. 897-924.

———— 1975, The thermodynamics of diffusion controlled metamorphic processes, *in* Cooper, A. R., and Heuer, A., eds., Mass Transport Phenomena in Ceramics: New York, Plenum Publishing Corp., p. 111-122.

Fletcher, R. C., and Hofmann, A. W., 1974, Simple models of diffusion and combined diffusion-infiltration metasomatism, *in* Hofmann, A.W., Giletti, B. J., Yoder, H. S., Jr., and Yund, R. A., eds., Geochemical Transport and Kinetics: Washington, D.C., Carnegie Inst. Washington, p. 243-259.

Frantz, J. D., 1974, Solubility constants in the system MgO–SiO_2–H_2O–HCl: Carnegie Inst. Washington Year Book 73, p. 380-384.

Frantz, J. D., and Eugster, H. P., 1973, Acid-base buffers: Use of Ag + AgCl in the experimental control of solution equilibria at elevated pressures and temperatures: Am. Jour. Sci., v. 273, p. 268-286.

Frantz, J. D., and Weisbrod, A., 1974, Infiltration metasomatism in the system K_2O–Al_2O_3–SiO_2–H_2O–HCl, *in* Hofmann, A. W., Giletti, B. J., Yoder, H. S., Jr., and Yund, R. A., eds., Geochemical Transport and Kinetics: Washington, D.C., Carnegie Inst. Washington, p. 261-271.

Garrels, R. M., and Christ, C. L., 1965, Solutions, Minerals, and Equilibria: New York, Harper and Row, 450 p.

Helgeson, H. C., 1971, Kinetics of mass transfer among silicates and aqueous solutions: Geochim. et Cosmochim. Acta, v. 35, p. 421-469.

Hofmann, Albrecht, 1972, Chromatographic theory of infiltration metasomatism and its application to feldspars: Am. Jour. Sci., v. 272, p. 69-90.

Katchalsky, A., and Curran, P. F., 1967, Nonequilibrium Thermodynamics in Biophysics: Cambridge, Mass., Harvard Univ. Press, 248 p.

Korzhinskii, D. S., 1959, Physicochemical Basis of the Analysis of the Paragenesis of Minerals: New York, Consultants Bur., 142 p.

———— 1970, Theory of Metasomatic Zoning: Oxford, Clarendon Press, 162 p.

Luce, R. W., Bartlett, R. W., and Parks, G. A., 1972, Dissolution kinetics of magnesium silicates: Geochim. et Cosmochim. Acta, v. 36, p. 35-50.

O'Neil, J. R., and Taylor, H. P., 1967, The oxygen isotope and cation exchange chemistry of feldspars: Am. Mineralogist, v. 52, p. 1414-1437.

Thompson, J. B., 1959, Local equilibrium in metasomatic processes, *in* Abelson, P. H., ed., Researches in Geochemistry, v. 2: New York, John Wiley & Sons, Inc., p. 427-457.

Weill, D. F., and Fyfe, W. S., 1964, The solubility of quartz in H_2O in the range 1000-4000 bars and 400-550°C: Geochim. et Cosmochim. Acta, v. 28, p. 1243-1255.

Wollast, R., 1967, Kinetics of the alteration of K-feldspar in buffered solutions at low temperature: Geochim. et Cosmochim. Acta, v. 31, p. 635-648.